

Assessment of Flow Over Periodic Hills using Scale Resolving Simulation (SRS) Methods

– Assignment 3 2023

Abhishek Dhiman, (abhdh352)
Tarun Teja, (tarna588)

1 Introduction

The phenomenon of turbulent separation from a curved surface & subsequent reattachment occurs in a large number of engineering problems, such as flow over the blades of a turbine, flow passing an obstruction in a pipe, and near an impeller in a mixing tank. The present study deals with a detailed analysis of flow over the periodic hill at $Re_H = 10595$ as this particular phenomenon is an established benchmark problem for the flow separation. The aim of the study is to evaluate the performance of two Scale Resolving Simulation (SRS) methods and perform validation against the Large Eddy Simulation (LES) data [1] for this benchmark problem.

In the periodic hill study, a well-defined flow passes over a series of hills, along a channel in a periodic fashion. As the flow passes over a hill, there is a pressure-induced separation from the curved surface. It then recirculates on the leeward face of the hill and reattaches at the base (valley) before accelerating up and over the next hill. This case consists of complex flow features such as the generation of an unsteady shear layer, re-circulation, strong pressure gradients, attached and detached boundary layers, and turbulence recycling due to the periodicity assumption.

Over the past few decades, the main research focus around the periodic hills simulation case has been on developing better wall functions and subgrid-scale models associated with hybrid RANS-LES models with a few studies using Scale-Adaptive Simulation (SAS) and more developed Stress-Blended Eddy Simulation (SBES) approach. It is observed that in many CFD simulations, RANS models show inherent technological limitations for certain types of flows and RANS models cannot always provide the degree of accuracy or the level of unsteady information during the design process. For this reason, there is an ongoing drive in the turbulence community to augment RANS capabilities by Scale-Resolving Simulation (SRS) methods. Since the resolution of the entire turbulent spectrum in the entire flow domain using direct numerical simulations (DNS) technique is computationally very expensive, the development and research in hybrid RANS-LES models is vital. These models only resolve parts of the turbulence spectrum or the turbulence is resolved in some part of the domain. Such methods are termed as Scale-Resolving Simulation (SRS) methods and the present study focuses on the SBES and SAS performance for periodic hill.

For free shear flows, it is often feasible to resolve the largest turbulent scales as they are of the order of the shear layer thickness. In the wall boundary layers, the turbulent eddies near the wall become very small relative to the boundary layer thickness and are more isotropic in nature, eventually dissipating into heat. These possess severe limitations for Large Eddy Simulations (LES) as the computational effort required is still far from the computing power available to the industry. Hence the need for hybrid models is increasing, where the large eddies are resolved away from walls and wall boundary layers are covered by established RANS models like $k - \omega$ SST.

2 Methodology

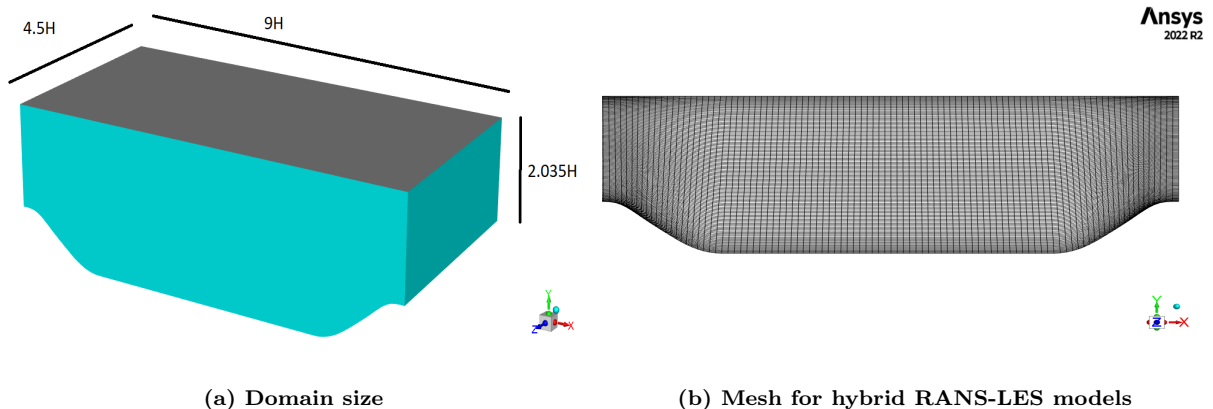
This section highlights the selection of domain size, mesh resolution, and iterative refinement in order to obtain a high-quality mesh for hybrid LES models. The mesh refinement is the verification process of mesh in that a few parameters like integral length scale are quantified, In detail explained in subsequent sections below.

2.1 Domain Size and Mesh Resolution

The domain size [9H x 4.5H x 2.035H], Fig.1a is based on the study conducted by Breuer [1]. The variable H represents the hill height, the span-wise extension is kept same as 4.5H and the domain height is reduced from 3.036H [1] to 2.035H in order to achieve high resolution for hybrid RANS-LES models and reduce computational costs. The stream-wise distance between the hills is kept to be 9H as recommended in [1] to enhance the stream-wise de-correlation to achieve a flow state independent of the inflow conditions.

The resolution of the mesh is significant to sufficiently resolve the energy contained in the larger eddies in the domain, Fig. 1b. The division of domain edges is iterative to achieve acceptable values of y^+ , x^+ , and z^+ . The nodes set of the edges in the y-direction are 130, with biasing near the top and bottom walls. The edge division in the x and z directions was kept uniform to 100 and 50 respectively. Thus obtaining 625779 cells in the domain, $y^+ = 2.18$, $x^+ = 23.16$ and $z^+ = 22.25$ based on the relation given by Eq. 1. The quantification of a good mesh resolution for LES type simulation is done in [2] which required $y^+ = 2$ and $x^+ = z^+ <= 20$ acceptable deviation of higher values possible. The $y = 4.5e - 3$, $x = 4.78e - 2$, and $z = 4.59e - 2$ are obtained from the final mesh used for hybrid RANS-LES models.

$$\frac{y^+}{y} = \frac{x^+}{x} = \frac{z^+}{z} \quad (1)$$



2.2 Boundary Conditions and Solver Setup

The simulations are carried out using Ansys Fluent (v2022 R2). The considered fluid is air with density (ρ) = 0.195 [kg/m³] and dynamic viscosity (μ) = 1.84e⁻⁵ [Pas]. The stream-wise and span-wise boundaries are initialized with periodic conditions with a pressure gradient (dp/dx) = -0.02262 [Pa/m] to achieve the $R_{eH} = 10595$. The top and bottom boundaries are initialized with no-slip wall boundary conditions. The convergence criteria are initially set to be 10^{-5} and all the continuity and velocity residuals are reduced to 10^{-3} for the RANS precursor part. But for SBES and SAS, the residual showed oscillations, highest shown for continuity residual which oscillated between ($10^{-1} - 10^{-2}$) whereas other residuals were observed to be oscillating well below 10^{-3} .

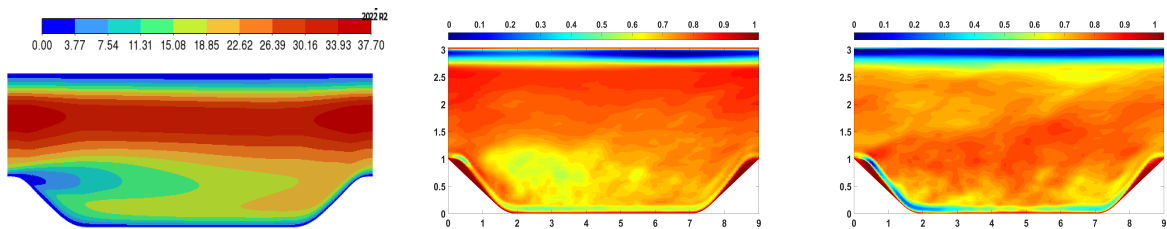
Both the hybrid models (SAS and SBES) have pressure-based, steady RANS results with k - ω SST model results as base solution which post-convergence switched to SAS and SBES. The RANS model used coupled solver for pressure-velocity coupling, a least square cell-based approach for spatial gradients, a second-order scheme for pressure and momentum terms, and lastly second-order upwind scheme for turbulent kinetic energy and dissipate rate.

Once the RANS solution is converged, the model is switched to SBES with Wall Adapting Local Eddy Viscosity (WALE) as a sub-grid model [3]. The motivation behind the selection of WALE is a good estimation of wall asymptotic behavior for wall-bounded flows and correction treatment of laminar zones of the domain by returning zero turbulent viscosity for laminar shear flows regions [3]. The pressure-velocity coupling is handled with Non-Iterative Time Advancement (NITA) with fractional steps to speed up the transient simulation [3]. The spatial discretization for pressure and momentum is selected as Standard and Bounded Central Differencing respectively and keeping the rest setting the same as RANS.

Similarly, the same steps are followed for SAS where WALE is not applicable but the rest of the setting remains the same. The time step size ($\Delta t = 0.0956$) is estimated using Eq. 2 assuming $CFL = 1$, $U_{bulk} = 0.9997$ [m/s], $\Delta x = 0.09557$. But later during the solution phases, the time step is reduced to 0.01 (SBES) and 0.005 (SAS) to keep the max CFL in the entire domain below 0.8 and 0.5 respectively [4]. **Note:** While starting the SAS simulation it was observed that due to the converged solution for RANS, the initial unsteadiness was not present. To tackle the problem, first, the TUI command (/solve/initialize/init-turb-vel-fluctuations) was executed, then RANS was switched to SBES for two flow through, and eventually, the solution was switched to the SAS model.

$$CFL = \frac{U_{bulk} * \Delta t}{\Delta x} \quad (2)$$

2.3 Mesh Verification



(a) RANS: Integral length (l_o/Δ) (b) SBES: TKE spectrum, ($> 70\%$) (c) SBES: LESIQ_v (> 0.8) [5]
Figure 2: Mesh resolution w.r.t l_o/Δ , ratio of resolved/total TKE and LES index of quality (LESIQ_v)

Multiple methods are followed for the mesh verification process i.e. integral length scale (l_o/Δ) for precursor RANS Fig. 2a, the ratio of resolved Turbulent Kinetic Energy (TKE) to total (resolved + modeled) for SBES 2b using Eq. 3, LES index of quality 2c proposed by Celik [5] using Eq. 4 and the two-point correlation Fig. 3 method suggested by Lars [6] as a good method to estimate mesh resolution for SBES and SAS models.

$$CFL = \frac{0.5 * (u' u'^2_{rms} + v' v'^2_{rms} + w' w'^2_{rms})}{(0.5 * (u' u'^2_{rms} + v' v'^2_{rms} + w' w'^2_{rms})) + (\mu_{turb}/(\rho * 0.325WALE * CellVolume^{1/3}))^2} \quad (3)$$

$$\text{LESIQ}_v = \frac{1}{1 + 0.05 * ((\mu_{molecular} + \mu_{turb})/\mu_{turb})^{0.53}} \quad (4)$$

Fig. 2a shows the domain which indicates the region of resolved TKE based on the ($l_o/\Delta > 4.8$) i.e approx 5 cells to resolve 80% TKE [2]. Near the top and bottom walls, the mesh resolution indicates lesser resolved TKE. Checking the same mesh w.r.t the ratio of resolved/(resolved + modeled) spectrum shows that the resolved TKE is more than 76% in the entire domain except close to the top wall Fig. 2b. Next is the LESIQ_v proposed by Celik [5] which is a dimensionless number between zero and one where values greater than 0.8 are considered good for LES. Fig. 2c

shows that the entire domain has a good resolution (> 0.8) for LES. Hence, the mesh resolution is good for hybrid RANS-LES models as well.

Next is the two-point correlation method in Fig. 3 is only performed for stream-wise direction. where the fluctuating component of the instantaneous velocities $[u', v', w']$ is at 5 incremental locations close to the inlet. These locations are the center of cells i.e [1st, 3rd, 5th, 7th, 9th] are monitored on the center plane and two equidistant planes from center plane for averaged u' correlation. The first point is placed at the cell center of 1st cell i.e. $\Delta x/2$ in all three planes. The subplots [1, 2, 3] show that the correlation drops from the center of 1st cell to 3rd for u', v', w' respectively. The drop is sufficiently low to be considered as De-Correlated for both SBES and SAS models implying the mesh resolution is sufficiently fine for LES and hybrid RANS-LES models. Similarly, three planes are created in the domain equally distant from the center plane and the u' is evaluated and averaged. The result is shown in Fig. 3 subplot 4, showing the De-Correlation < 0.4 from the center of 1st cell to the center of 9th cell. Hence, the mesh is evaluated to be sufficiently fine for hybrid RANS-LES models (SBES and SAS) for further analysis in this study.

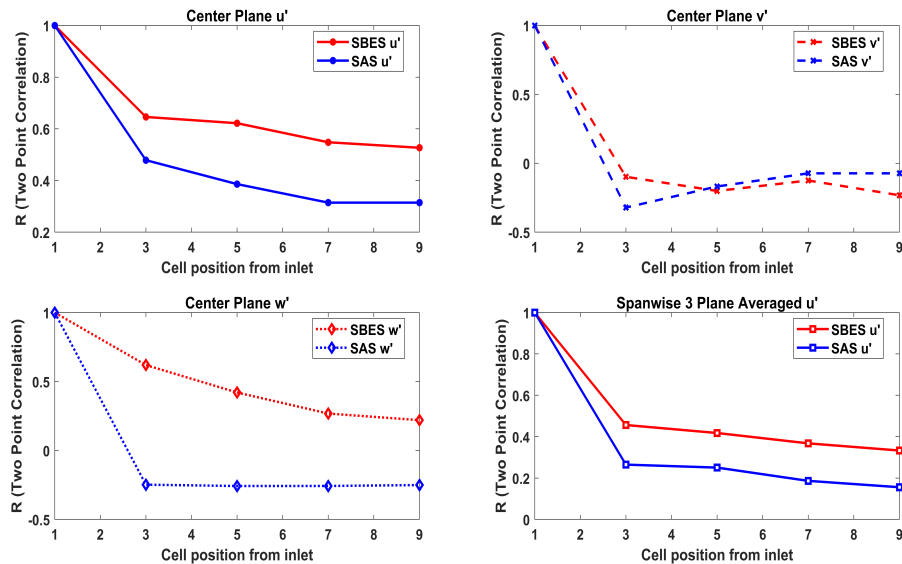


Figure 3: Stream wise instantaneous velocities correlation ($\Delta x = 0.9557$)

2.4 Statistical Convergence and Sampling Error

Statistical convergence in Scale Resolving Simulation (SRS) is associated with two sources of uncertainties i.e. the influence of initial transient and statistical error due to finite number of samples [7]. The present study followed the procedure to identify and quantify the two sources of errors w.r.t SRS models as presented in [7]. The data sampling is performed for 13 flow-through (flow parameters mentioned below) in order to estimate the initial transient point and quantification of MSE for sampling error. Post MSE quantification, the data is sampled for 15 flow through for further analysis of velocity profiles, pressure distribution, wall shear distribution, fluctuating velocity component profiles ($u' \& v'$), and Reynolds shear stress ($u'v'$).

Step 1: The initial transient identification and removal from the sample data are important in the quantification of statistical convergence of simulation, for which the Marginal Standard Error Rule (MSER) is used [7]. The visual estimation of statistical convergence is prone to human error and varies significantly leading to inconsistency in obtained results. The procedure followed in the present study identifies a truncation point that minimizes the width of the confidence interval about the truncated sample mean, Equation [1, 2] [7]. For SBES and SAS models, area-averaged

wall shear X, span-wise center plane average velocity, and velocity u at 5 stream-wise locations $x/H \in [0.05, 1, 2, 4, 6, 8]$ are monitored. After detecting the transient point, the sampled data till this point is removed and the rest of the data is used to quantify the sampling error.

The sampling error is estimated with an approach based on the direct estimation of sampling error for correlated data as the samples obtained from the SRS are generally not independent they represent the temporal evolution of Navier-Stokes equations [7]. The Equation [4] [7] are utilized for the quantification of MSE for each flow parameter presented in Table. 1.

Table 1: Statistical convergence of sampled data (Mean Squared Error (MSE)) after removing initial transient. Note: W-S X = Wall Shear X; SB = SBES; SA = SAS; (N) = Flow throughs

Parameter	SB(5)	SA(5)	SB(10)	SA(10)	SB(15)	SA(15)	SB(20)	SA(20)
Pressure	4.16e ⁻⁹	9.86e ⁻⁹	3.03e ⁻⁹	2.74e ⁻⁹	2.11e ⁻⁹	2.68e ⁻⁹	2.45e ⁻⁹	3.34e ⁻⁹
W-S X	3.12e ¹²	2.56e ⁻¹³	8.52e ¹⁴	7.29e ⁻¹⁴	4.62e ⁻¹⁴	6.53e ⁻¹⁴	4.76e ⁻¹⁴	1.22e ⁻¹³
u (0.05)	4.85e ⁻⁹	1.38e ⁻⁸	2.27e ⁻⁹	2.81e ⁻⁹	6.24e ⁻⁹	2.21e ⁻⁹	8.15e ⁻⁹	5.46e ⁻⁹
u (4)	2.15e ⁻⁹	6.12e ⁻⁹	1.04e ⁻⁹	1.22e ⁻⁹	2.80e ⁻⁹	9.89e ⁻¹⁰	2.45e ⁻⁹	2.46e ⁻⁹
u (8)	3.04e ⁻⁹	8.49e ⁻⁹	1.35e ⁻⁹	1.57e ⁻⁹	3.83e ⁻⁹	1.38e ⁻⁹	5.10e ⁻⁹	3.46e ⁻⁹
v (0.05)	1.29e ⁻⁷	5.77e ⁻⁸	5.84e ⁻⁸	5.82e ⁻⁸	3.96e ⁻⁸	3.58e ⁻⁸	3.24e ⁻⁸	2.74e ⁻⁸
v (4)	2.14e ⁻⁷	2.09e ⁻⁷	1.23e ⁻⁷	1.05e ⁻⁷	7.62e ⁻⁸	7.50e ⁻⁸	6.40e ⁻⁸	5.76e ⁻⁸
v (8)	2.31e ⁻⁷	1.91e ⁻⁷	9.67e ⁻⁸	1.14e ⁻⁷	6.76e ⁻⁸	7.65e ⁻⁸	5.57e ⁻⁸	6.13e ⁻⁸

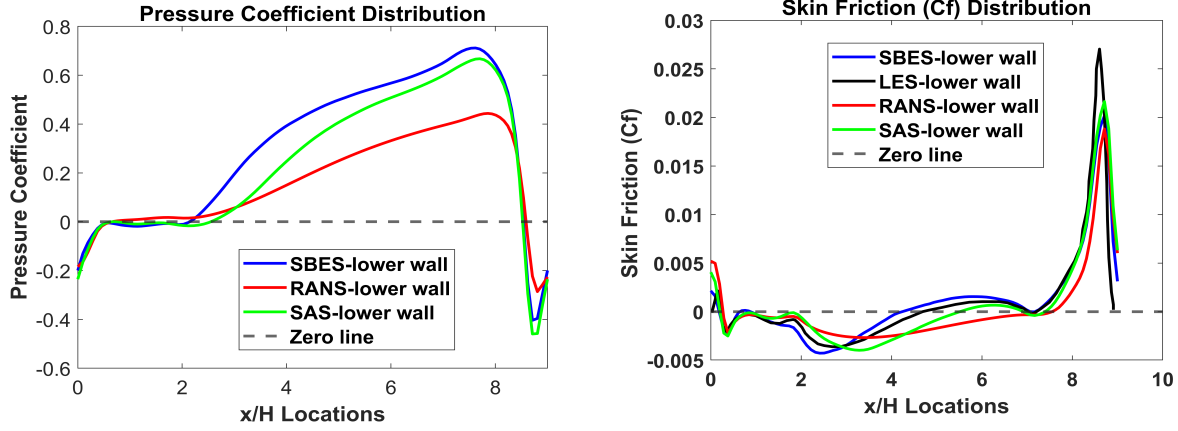
2.5 Post Processing Note

Similar to pressure and wall shear X, the velocity and Reynolds stress profiles are plotted in the stream-wise planes at locations $x/H \in [0.05, 1, 2, 4, 6, 8]$. These planes plot 50 line profiles which are averaged to get the final profile. This method results may result in undesirable wiggles/skipes in the profiles which were observed during this study as well and corrected during post processing using MATLAB scripts. Hence, the post-processing correction are required to capture smooth profiles at vertical lines at the above-mentioned locations.

3 Results

The results are validated against the more resolved LES data by Breuer [1] available at [8], [9]. The averaged pressure distribution on the bottom wall (hill-valley) is shown in Fig. 4a. The pressure validation data for LES was difficult to extract hence the comparison is made between the RAS, SBES, and SAS which followed the similar behavior reported by Breuer [1]. The initial negative pressure is from the pressure gradient applied on the periodic wall, after which the pressure plateau can be observed at the zero line which covers the major portion of re-circulation.

This pressure plateau is due to the re-circulation zone formation as the flow detaches from the hill and re-attaches in the valley. The near hill pressure distribution ($0 < x/H < 2$ and $8 < x/H < 9$) is captured well by the three models and shows a similar resemblance as captured in Breuer [1]. The pressure rise in the re-circulation region and re-attachment in the valley ($2 < x/H < 7.5$) is significantly different for all three models, where SAS catches up to SBES estimations ($6 < x/H < 7.5$). The peak value estimated by SBES and SAS at ($x/H \simeq 7.5$) shows good agreement but is underestimated by the RANS model.



(a) Pressure Coefficient Distribution (b) Skin Friction (C_f) Distribution
Figure 4: Averaged coefficient comparison plots on the lower wall for LES, SBES, SAS, and RANS

In the case of averaged skin friction coefficient (C_f), Fig. 4b, the separation points are captured well by all models w.r.t LES. The re-attachment location (C_f change signs from - to +) estimated by SBES (4.26) and LES (4.69) are in good agreement, whereas SAS (5.52) estimates a slightly larger zone and RANS (7.54) shows a significant jump in estimation. Contrary to re-circulation length, the sharp rise in C_f and peak value ($7 < x/H < 9$) is well captured by RANS and SAS w.r.t LES and highlights its abilities in the wall regions. The SBES significantly underestimates the peak C_f value but shows good agreement in the near region. A small re-circulation zone is captured by SAS aft the flow re-attachment at ($6.9 < x/H < 7.3$) at the start of the second hill.

The velocity U profiles at different x/H line locations in the span-wise center plane are shown in Fig.5. The 6 stream-wise locations are considered such that the first 4 locations [0.05, 1, 2, 4] cover shear layers and re-circulation zone, and the last two locations [6, 8] are at the end of re-circulation and outlet respectively. At all 6 locations, the SBES and LES results are in great agreement and overlapping. All SAS profiles show slight under-estimation near the top and bottom wall. RANS on the other hand displays good near wall estimation, over-estimation in peak values at all locations and fails to predict the profiles away from the wall, Fig. 5.

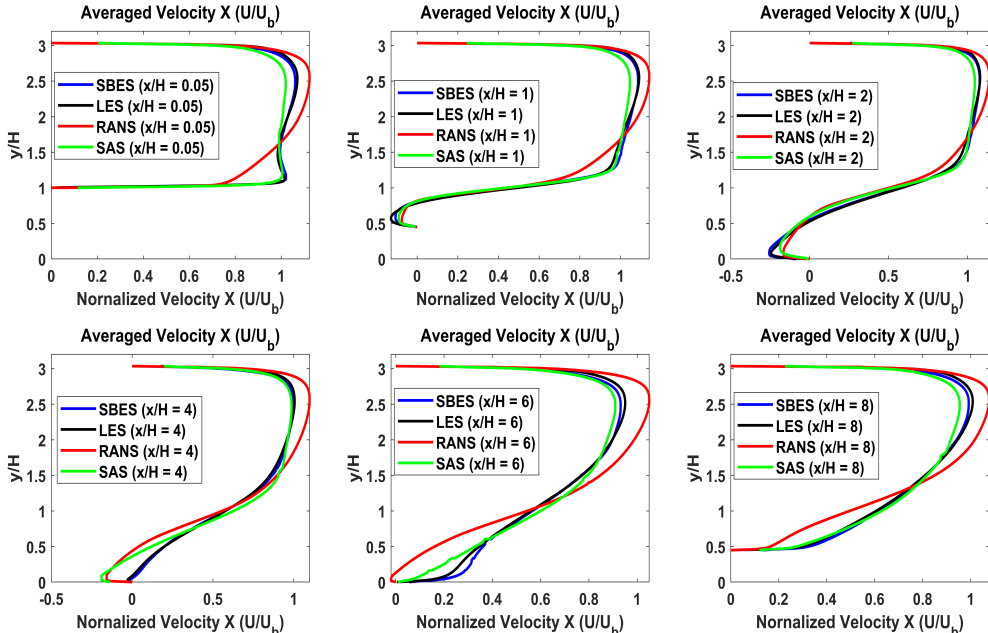


Figure 5: Velocity U profiles at different locations for Various Turbulence models

The velocity V profiles, Fig. 6 shows good agreement with LES at different locations. The SBES and LES are in good agreement at $x/H \in [1, 2, 6, 8]$, significant over-estimation near inlet, in re-circulation and outlet i.e. $x/H \in [0.05, 4, 8]$ respectively, with significant deviations at $[0.05, 5]$. The entire SAS and SBES profiles are in good at $x/H \in [1, 4]$. The SAS model profile agreed well with LES only at $x/H = 8$ i.e. near the outlet and failed to give any good predictions at other locations. The RANS model predictions are satisfactory at $x/H \in [1, 6]$ and way off at other locations. An important observation is the magnitude of the V/U_b is significantly smaller than U/U_b at all 6 locations.

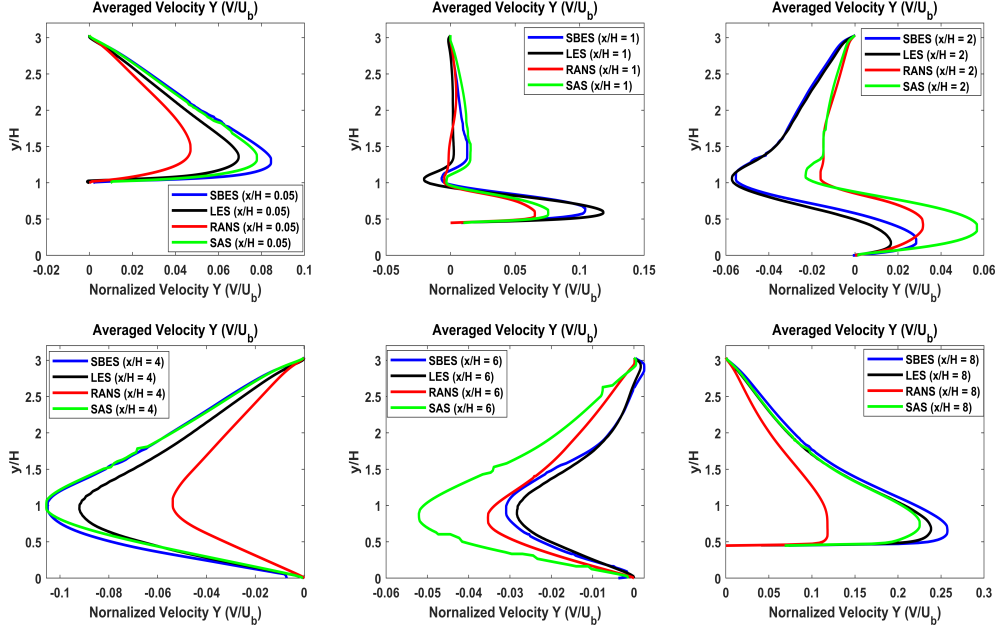


Figure 6: Velocity V profiles at different locations for Various Turbulence models

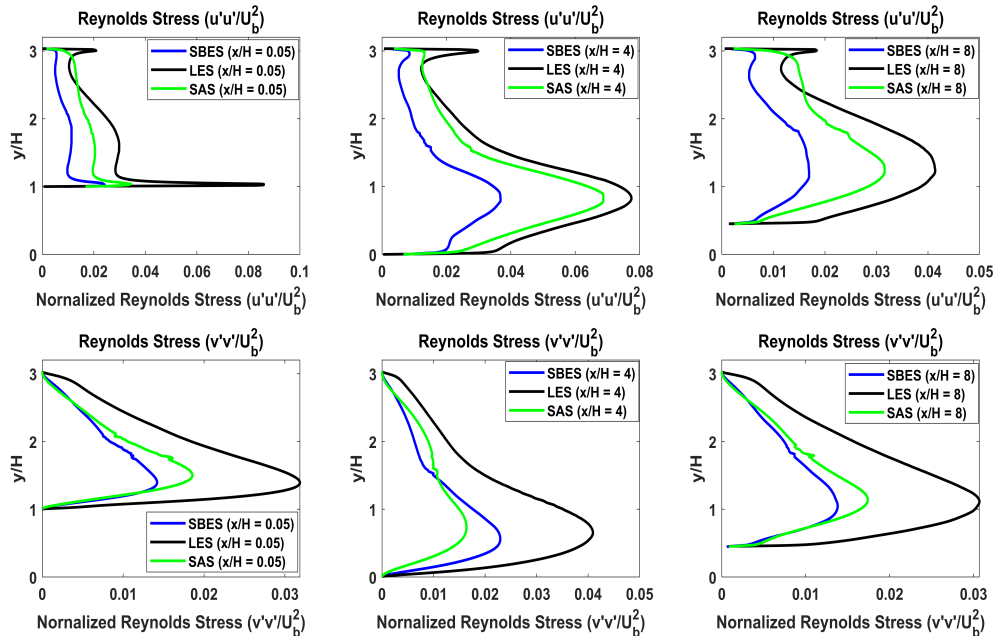


Figure 7: Reynolds shear stress ($u'u'$ & $v'v'$) $Re = 10595$ compared against the LES data

The normal Reynolds stress ($u'u'$ and $v'v'$) are plotted at three locations $x/H \in [0.05, 4, 8]$ Fig. 7, close to inlet, center, and close of the outlet of the domain as mentioned in 2.5 similar to (U and V) velocities. The Reynolds stress ($u'u'$) for SAS agrees well with the benchmark

LES data at $x/H = 4$ trend, especially the peak value. Majorly, significant under-estimation is predicted by both SAS and SBES at all locations but follows the same profile as LES Fig. 7 subplot [1, 2, 3]. Similarly for $(v'v')$, Fig. 7 subplot [4, 5, 6] shows the normal stress which is considerably under-predicted by both models in the shear layer region ($1 < y/H < 2$) at $x/H = 0.05$. The peak values are poorly captured at all three locations w.r.t LES. In essence, the $v'v'$ estimation is poor at all 3 locations by SAS and SBES.

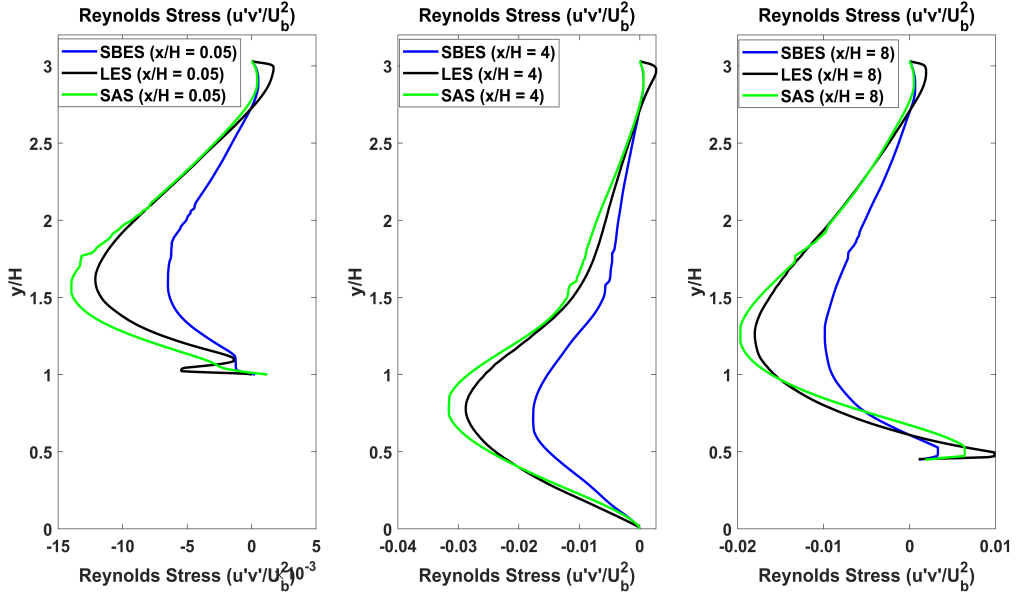


Figure 8: Reynolds shear stress $(u'v')$ $Re = 10595$ compared against the LES data

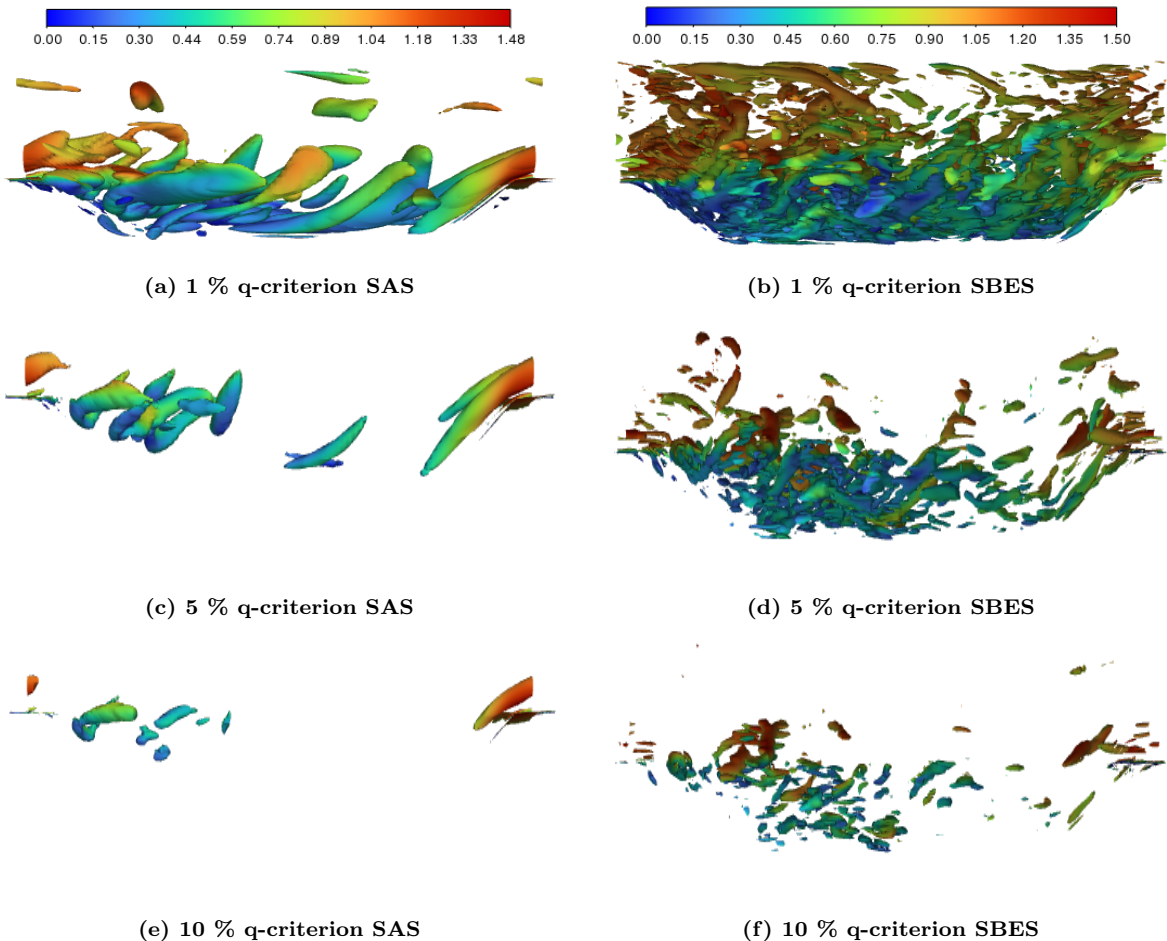


Figure 9: Velocity magnitude q-criterion for on iso-surfaces for difference % of positive range

The Reynolds shear stresses ($u'v'$) profiles for the same locations as $u'u'$ and $v'v'$ can be seen in Fig. 8. The obtained results from the SAS model are showing great similarity (almost overlapping) with LES data at all locations. But a closer look at the near wall region shows that the profile is not well captured by SAS. Coming to SBES, poor agreement is observed at all three locations. At $y/H > 2$ the trend and agreement are good w.r.t LES. The peak values predicted by SBES are significantly under-predicted in all the profiles, Fig. 8.

Q -criterion is used for the visualization of coherent vortical structures in the domain flow resolved by SAS and SBES model, Fig. 9. The q -criterion is the second invariant of the velocity gradient tensor where the positive range quantifies the domain area dominated by vorticity and negative range implies area dominated by strain rate or viscous tensor.

The q -criterion are created on the iso-surfaces 1%, 5% and 10% of the positive range and the contours are presented for velocity magnitude on these iso-surfaces for SAS and SBES, Fig. 9. Firstly, the 1% case for SAS (Fig. 9a) and SBES (Fig. 9b) shows scale of the turbulent vortical structures captured by SBES. It is able to capture small and large structures near wall and away from wall region respectively, where as SAS is only able to estimate very large structures away from the wall. Secondly, the 5% case shows the reduction in vortical structures as expected but SBES (Fig. 9d) is again able to resolve a good scale of structure and SAS (Fig. 9c) lacks the same ability. Finally, for 10% case the trend of reducing quantification remains the same for both SBES and SAS, where SBES now captures only small structures as the larger ones are not present in the domain at 10% of positive range.

4 Discussion

The observation of a small re-circulation captured by SAS (Fig. 4b) at $(6.9 < x/H < 7.3)$ is also documented in Breuer [1] at $(7 < x/H < 7.4)$ for $R_e > 200$ with the largest size observed at $R_e = 2800$. This implies that the size of this tiny re-circulation zones reduces for $R_e > 2800$ as the flow attachment increases with R_e [1]. But in the present study only $R_e = 10595$ is simulated hence the size comparison is not performed. The flow separation is well capture by all three models especially SBES which agrees well with LES profile in Fig. 4b. The pressure distribution trend displayed in Fig. 4a by SBES is visually more similar to LES [1].

The magnitude of velocity U (Fig. 6) component is significantly lower than the velocity U (Fig. 5) in the stream-wise direction which is also observed in [1]. The performance of RANS in free shear flow (as in this study) is non uniform [4] which can be seen as the deviations away from the wall in U and V velocity profiles. The SBES stream-wise velocity (U) profiles are in complete agreement with LES at all locations, Fig. 5 signifying the the SBES shielding function capability to explicitly switch between RANS and LES mode where the modelled portions are based on eddy viscosity concept [4]. The SAS model also show great agreement against LES with marginal deviations Fig. 5. The grid used in the study is coarser w.r.t to the LES requirements which turned out to be plus point for the SAS model that can be run for wider range of numerical grids. The SAS results obtained for stream-wise velocity component and the resolved structures are satisfactory.

The velocity V component profiles showed by SBES models out performed SAS at different locations and SBES agreed well with LES, Fig. 6. The velocity V component itself is sensitive [1] compared to velocity U component. The SBES profiles are well captured in the re-circulation zone i.e. $x/H \in [1, 2, 4]$ due to the Wall Modelled LES (WMLES) which uses RANS for inner most part of boundary layer and LES in the main boundary layer [4].

The normal Reynolds stress component ($u'u'$ & $v'v'$) profiles in Fig. 7 highly under-predicts the magnitude at all three locations i.e shear layer, re-circulation zone and re-attachment region. The fruitful observation is the y/H positions of the peak values for $u'u'$ and $v'v'$ which is similar

to LES peak at $R_{eH} = 10595$ for both SAS and SBES models. The peak values move closer to the walls (here lower wall) as the R_{eH} increases as observed by Breuer [1]. The Reynolds shear stress agreement by SAS model is good which highlights its ability to work well with coarser grid, however the same ability is not shown by SBES model which requires comparatively higher resolution, Fig. 8. The SAS model continues the profile agreement with LES towards the bottom wall implying the strength of under-lying length scale adjustment based on the second velocity derivative for resolved structures [4].

The visualization from the Q-criterion, Fig. 9 shows the wide range of turbulent structure sizes captures by SAS and SBES. For the same percentage of vorticity [1%, 5% and 10%], the SBES resolved vast length scales in near wall region and in the main domain. Whereas the SAS model only resolved larger structures in the main domain and smaller vortex structures near the walls are not resolved. The larger and elongated stream-wise structures majorly captured by the SAS model on the concave wall on the second hill are also observed and discussed in Breuer [1] as type-b structures. The generation of these structures is either because of the instability due to effect of centrifugal forces or by the type-2 instability, where the inclination is towards the type-2 instabilities [1]. The structures observed for SAS at 5% (Fig. 9c) and 10% (Fig. 9e) are termed as type-c in Breuer [1] which develop in shear region due to Kelvin-Helmholtz instability [10]. These structures tend to change orientation from span-wise to stream-wise direction when convected downstream.

5 Conclusions

The present study aims to simulate the periodic hill turbulent flow case at $R_{eH} = 10595$. The analysis is performed using two SRS models (Hybrid RANS-LES) namely, SAS and SBES. The grid resolution with LES requirements is used to execute the simulation and obtain results for model comparison. The methodology followed for hybrid RANS-LES models with l_o/Δ , resolved TKE spectrum, LES Index of Quality and two point correlation is recommended to save computation time. The process followed for detection of statistical convergence and quantification of sampling error is simple, time inexpensive and recommended to prevent potential errors. The SBES results showed better agreement against LES data than SAS and the finding are in compliance with the existing literature [1]. The presence of re-circulation small re-circulation zone on the second hill ($6.9 < x/H < 7.3$) is confirmed for $R_{eH} = 10595$ by SAS model. The skin friction distribution and estimation of re-circulation zone length by SBES displayed complete agreement with LES, except the peak value. The SAS and SBES models showed complete agreement in capturing the velocity U at all locations against LES data. The Reynolds stress ($u'u'$ & $v'v'$) are under-predicted by SAS and SBES whereas $u'v'$ profiles are satisfactory. The recommended model is SBES with advantages of superior boundary layer shielding, transition between RANS to LES mode, WMLES capability.

References

- [1] M Breuer CRMM N Peller. Flow over periodic hills à Numerical and experimental study in a wide range of Reynolds numbers. 2008.
- [2] Gerasimov DA. Quick Guide to Setting Up LES-Type Simulations. 2015.
- [3] Ansys. Ansys Fluent Theory Guide. 2020.

- [4] Menter FR. Best Practice: Scale-Resolving Simulations in ANSYS CFD. 2015.
- [5] Johan Meyers PS Bernard J Geurts. Quality and Reliability of Large-Eddy Simulations. 12th ed. ERCOFTAC SERIES, SPRINGER, ISBN: 978-1-4020-8577-2; 2008.
- [6] Davidson L. Large Eddy Simulations: how to evaluate resolution. 2009.
- [7] Michael Bergmann GAEK Christian Morsbach. Statistical Error Estimation Methods for Engineering-Relevant Quantities From Scale-Resolving Simulations. 2021.
- [8] ERCOFTAC Knowledge Base: Abstr:2D Periodic Hill Flow;. Available from: https://www.kbwiki.ercoftac.org/w/index.php/UFR_3-30_Evaluation.
- [9] Turbulence Modeling Resource: LES: 2-D Periodic Hill (Langley Research Center);. Available from: https://turbmodels.larc.nasa.gov/Other_LES_Data/2dhill_periodic.html.
- [10] KelvinâHelmholtz instability;. Available from: https://en.wikipedia.org/wiki/Kelvin%20%93Helmholtz_instability.